Northern Hemisphere Summer Monsoon Singularities and Climatological Intraseasonal Oscillation

BIN WANG AND XIHUA XU

Department of Meteorology, School of Ocean and Earth Science and Technology, University of Hawaii, Honolulu, Hawaii

(Manuscript received 22 February 1996, in final form 9 September 1996)

ABSTRACT

Using climatological pentad mean outgoing longwave radiation (OLR) and European Centre for Medium-Range Weather Forecasts analysis winds, the authors show that the Northern Hemisphere summer monsoon displays statistically significant climatological intraseasonal oscillations (CISOs). The extreme phases of CISO characterize monsoon singularities—monsoon events that occur on a fixed pentad with usual regularity, whereas the transitional phases of CISO represent the largest year-to-year monsoon variations.

The CISO results from a phase-locking of transient intraseasonal oscillation to annual cycle. It exhibits a dynamically coherent structure between enhanced convection and low-level convergent (upper-level divergent) cyclonic (anticyclonic) circulation. Its phase propagates primarily northward from the equator to the northern Philippines during early summer (May–July), and westward along 15°N from 170°E to the Bay of Bengal during August and September.

The propagation of CISO links monsoon singularities occurring in different regions. Four CISO cycles are identified from May to October. The first cycle has a peak wet phase in mid-May that starts the monsoon over the South China Sea and Philippines. Its dry phase in late May and early June brings the premonsoon dry weather over the regions of western North Pacific summer monsoon (WNPSM), Meiyu/Baiu, and Indian summer monsoon (ISM). The wet phase of Cycle II peaking in mid-June marks the onsets of WNPSM, continental ISM, and Meiyu, whereas the dry phase in early to mid-July corresponds to the first major breaks in WNPSM and ISM, and the end of Meiyu. The wet phase of Cycle III peaking in mid-August benchmarks the height of WNPSM, which was followed by a conspicuous dry phase propagating westward and causing the second breaks of WNPSM (in early September) and ISM (in mid-September). The wet phase of Cycle IV represents the last active WNPSM and withdrawal of ISM in mid-October.

The relationships among ISM, WNPSM, and East Asian Subtropical Monsoon (EASM) are season dependent. During Cycle II, convective activities in the three monsoon regions are nearly in phase. During Cycle III, however, the convective activities are out of phase between ISM and WNPSM; meanwhile, little linkage exists between WNPSM and EASM. The causes of unstable relationships and the phase propagation of CISO are discussed.

1. Introduction

The Northern Hemisphere (NH) summer monsoon is a primary component of the global climate system. In the literature, regional monsoon components in the NH have been named somewhat differently. To avoid confusion, we define NH summer monsoon as consisting of three major regional components: the Indian Summer Monsoon (ISM), east Asian Subtropical Monsoon (EASM), and western North Pacific Summer Monsoon (WNPSM). Previous studies have summarized major circulation systems associated with ISM (Krishnamurti 1985), EASM (Tao and Chen 1987; Ninomiya and Murakami 1987), and WNPSM (Murakami and Matsumoto 1994). The WNPSM and ISM are tropical monsoons characterized by 1) low-level monsoon troughs and associated southwesterlies equatorward side of the troughs and northward cross-equatorial flows, and 2) upper-tropospheric easterlies to the south of the subtropical ridge. The vertical shear of zonal flows provides a meaningful measure of the strength and extent of the tropical monsoon (Webster and Yang 1992). The EASM, on the other hand, is characterized by 1) a low-level convergence zone between southerlies from the Tropics and weak northerlies from the midlatitudes, and 2) upper-tropospheric westerlies north of the subtropical ridge.

The Northern Hemisphere summer monsoon is well known for its prominent subseasonal variation—the active and break monsoons (Krishnamurti and Bhalme 1976; and many others)—and the abrupt changes during its seasonal march. The active/break monsoons and the alternation between sudden changes and steady evolution are directly associated with intraseasonal oscillations that are widely observed in the ISM (e.g., Yasunari

Corresponding author address: Dr. Bin Wang, Department of Meteorology, University of Hawaii, 2525 Correa Road, Honolulu, HI 96822.
E-mail: bwang@soest.hawaii.edu

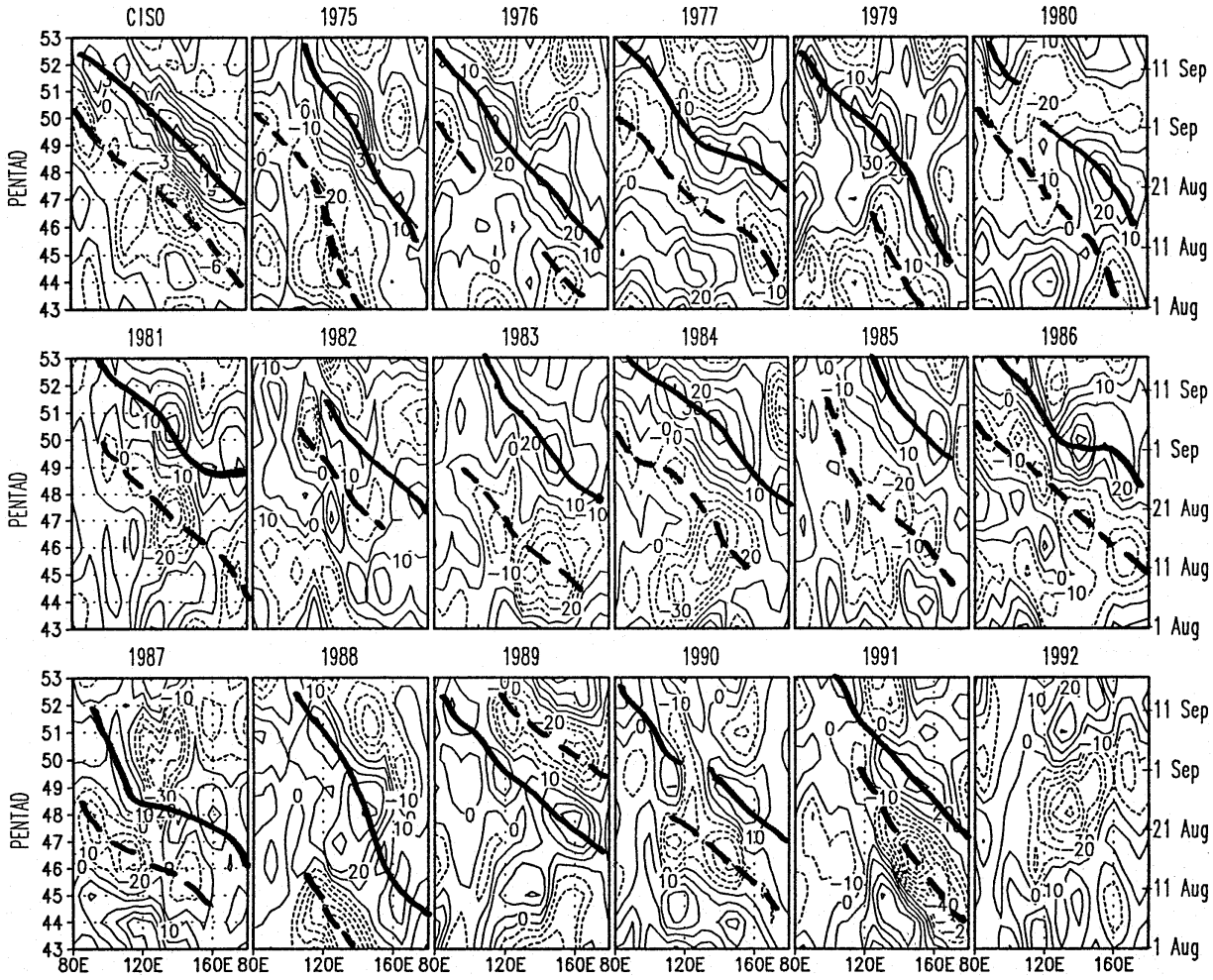

FIG. 1. The time–longitude diagrams of 20–72-day OLR anomalies along 12.5°–22.5°N for the period of 1 August–15 September. The 18 panels are for climatological mean (CISO) and each individual year from 1975 to 1992 (1978 missing). The thick dashed and solid lines outline, respectively, the wet and dry phases of westward propagating episodes. The CISO emerges as a result of the phase locking of transient ISOs to the annual cycle.

1979, 1980; Sikka and Gadgel 1980; Krishnamurti and Subrahmanyan 1982; and others), the EASM (e.g., Chen and Jin 1984; Lau and Chan 1986), the WNPSM (e.g., Chen and Murakami 1988; Huang 1994), and the Australian summer monsoon (e.g., Murakami et al. 1986; Holland 1986; McBride 1987; Hendon and Liebmann 1990). The alternation between abrupt changes and steady evolution is particularly evident in the EASM. Abrupt northward advance of the Meiyu front occurs normally in mid-June and mid-July (Tao and Chen 1987; Ding 1992; Tanaka 1992). Matsumoto (1992) used ''discontinuities'' (or ''jumps'') to characterize subseasonal variations of monsoon. Ueda et al. (1995) showed that the abrupt northward shift of convective anomalies over the western Pacific around 20°N, 150°E in late July is accompanied by a sudden appearance of large-scale cyclonic circulations and by changes in tropical cyclone tracks. The causes of the abrupt changes were speculated but not well understood. Further studies in this regard are much needed.

Our knowledge on the interaction between tropical intraseasonal oscillation (ISO) and monsoons has expanded rapidly in the last decade or so (Wang and Ding 1992). On the one hand, transient ISOs are responsible for active/break monsoons. On the other hand, the annual cycle modulates ISO intensity (e.g., Madden 1986), movement (Wang and Rui 1990; Zhu and Wang 1993), and frequency (Hartmann et al. 1992).

A prominent feature of monsoon (annual cycle)–ISO interaction is that the annual variation of general circulation tends to regulate phase propagation of tropical ISO. Figure 1 shows a set of longitude–time diagrams of OLR pentad mean anomalies (subjected to a 20–72-day filtering) along 15°–20°N. Notable westward propagation episodes tend to repeat themselves during about the same period of the calendar year. The phase-locking

of ISOs to the annual cycle results in a significant westward propagating climatological intraseasonal oscillation (CISO), which is in turn responsible for subseasonal variation of summer monsoons.

The extremely wet and dry phases of CISO imply climatological active and break monsoons, respectively. We refer to the peak active/break monsoons that occur on or near a fixed pentad with usual regularity as summer monsoon singularities. For instance, at 140°E and 15°–20°E (the core region of the WNPSM), dry anomalies occur at pentad 49 (August 29–September 2) on a regular basis, forming a climatological break monsoon singularity (Fig. 1). In this paper, we will show that the presence of climate singularities is one of the fundamental characteristics of the NH summer monsoon.

Questions arising here include: 1) to what extent are transient ISOs controlled by the annual cycle in NH summer monsoon domain? Is the phase locking of ISOs to annual cycles and resulting monsoon singularities statistically significant and physically meaningful? 2) How are monsoon singularities distributed spatially and temporally? Are they related to each other? If so, how are they related? 3) What physical processes possibly determine the movement of CISO and the linkage among monsoon singularities over different regions? The present paper is aimed at addressing and discussing these questions.

We will describe the data and define CISO first in section 2 and then demonstrate, in section 3, the statistical significance of the NH summer monsoon singularities associated with the extreme phases of CISO. The spatial and temporal distributions of the summer monsoon singularities occurring in various monsoon regions are then conveniently studied by examining the behavior of CISO. In sections 4, 5, and 6 we analyze, respectively, the dynamic structure, the propagation, and the life cycle of CISO and the relationship among the singularities in the three major NH summer monsoon components. The possible causes for the CISO propagation and monsoon singularities are discussed in the last section.

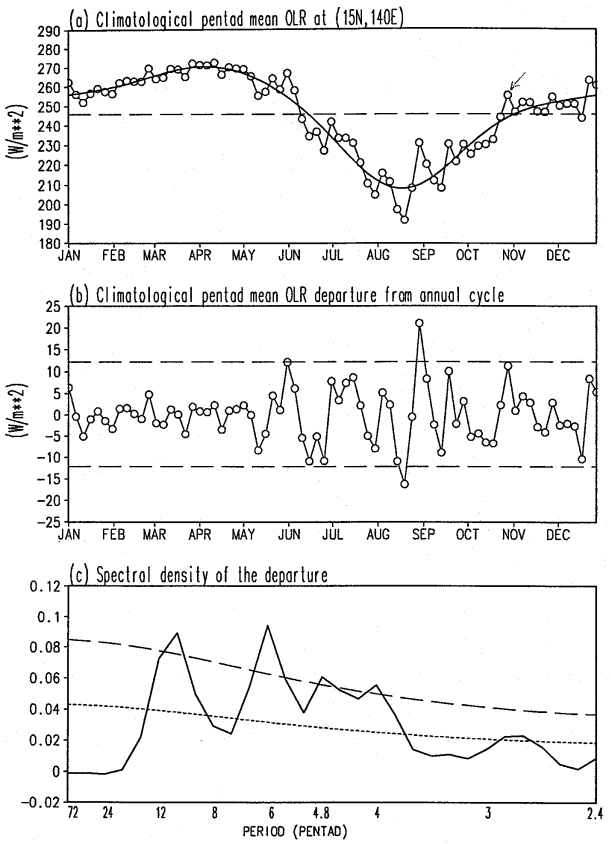

FIG. 2. (a) Climatological pentad mean OLR at 15°N, 140°E and the base annual cycle (heavy line) defined by the sum of its first four Fourier harmonics. The onset, peak, and withdrawal of summer monsoon rainfall are marked. (b) The climatological pentad mean OLR departure from the base annual cycle. The dashed lines show the upper and lower bounds of the mean plus two standard deviations. (c) The spectral density of the departure. The dashed and dotted lines denote the upper and lower bounds of the 95% confidence interval against a red noise background.

2. Data and the definition of CISO

a. Data

The primary dataset used in the present analysis is satellite-derived outgoing longwave radiation (OLR). Regardless of their flaws in estimating deep convection, the OLR can, nevertheless, offer reasonably good estimates for deep convection and rainfall in most tropical regions when cautions are exercised (for a detailed discussion refer to Wang 1994). In view of the thermally driving nature of the tropical general circulation, deep convection is a key parameter for highlighting the energy source that drives tropical atmospheric motion. To describe subseasonal climatic variations, adequate time resolution, such as pentad mean, are needed. To make a statistically meaningful climatology, long records are also desirable. The OLR data available to us cover 17 yr (from 1975 to 1992 with 9 months missing in 1978). These climatological pentad mean time series are bases for the present analysis. In addition to the OLR data, climatological pentad mean winds derived from European Centre for Medium-Range Weather Forecasts (ECMWF) global analysis for the period of 1979–1993 are also used. Both the OLR and ECMWF data are made in 5° lat × 5° long grids. The analysis domain spans 70°E–170°W and 10°S–40°N.

b. The definition of CISO

The climatological pentad mean OLR time series in NH summer monsoon region show considerable fluctuations on intraseasonal timescales. Figure 2a presents an example for the core region of WNPSM at (15°N, 140°E). To examine the nature of the fluctuation, we removed the first four Fourier harmonics (a smoothed annual variation) from the climatological pentad mean

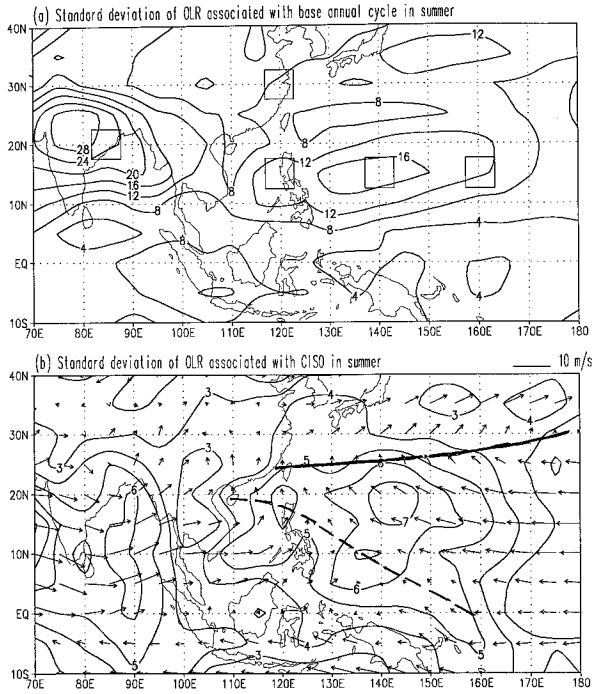

FIG. 3. (a) Standard deviation of the base annual cycle of OLR (W m^{-2}) in northern summer from May to October. The five boxes indicate the locations for which CISO OLR are shown in Fig. 6. (b) Same as in (a) except for the Climatological Intraseasonal Oscillation (CISO) component of OLR. Arrows show summer mean 850-hPa winds. Heavy solid and dashed lines outline the positions of subtropical ridge and monsoon trough, respectively.

series. The resultant departure shown in Fig. 2b displays oscillatory behavior with considerable amplitude from May to November. The spectrum of the departure time series reveals a concentration of variance on a broad timescale ranging from 20 to 60 days with the most prominent peak occurring at 30 days and the second peak at about 50–60 days (Fig. 2c). There is another weaker peak at 20–25 days. All three peaks are statistically significant against a red noise background at 95% confidence level.

The results shown in Fig. 2 suggest that the climatological pentad mean OLR contains two major components, a ''smoothed'' base annual cycle and a climatological intraseasonal oscillation. To quantify these two components, we partition climatological pentad mean series $[y_c(i), i = 1, 73]$ into three components by Fourier analysis:

$$y_c(i) = y_{ca}(i) + y_{ciso}(i) + R(i), \qquad (2.1)$$

where y_{ca} denotes the sum of the first four Fourier harmonics (period longer than 3 months), y_{ciso} represents the sum of the 5th to 18th harmonics (period ranging from 20 to 73 days), and R the residual. Hereafter, we will refer to the smoothed annual cycle y_{ca} as base annual cycle and y_{ciso} as a CISO, respectively.

From Fig. 2, we note that both the onset in mid-June and the peak in mid-August of the WNPSM coincide

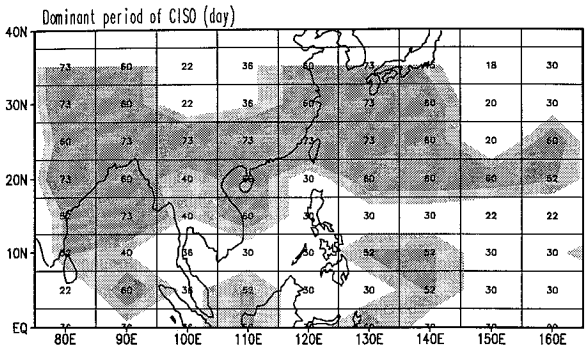

FIG. 4. Spatial variation of the dominant period of CISO in units of days. Dark and light shadings represent areas where CISO period is longer than 50 days and between 40 and 50 days, respectively.

precisely with the two corresponding wet extrema of CISO. The withdrawal at the end of October and two major breaks in mid-July and early September are also associated with corresponding dry extrema of CISO. This indicates that CISO depicts characteristic evolutions of summer monsoons. Therefore, monsoon singularities can be studied by examining extreme phases or sudden changes of CISO.

The CISO can also be viewed as one component of transient ISO that is phase-locked to the annual cycle. The transient ISO (period ranging from 20 to 73 days) may then be considered as a sum of the CISO and a departure from CISO, namely,

$$y_{iso}(j) = y_{ciso}(j) + y'_{iso}(j). \qquad (2.2)$$

The departure $y'_{iso}(j)$ represents the ISO component that is not phase locked to the annual cycle or that results from the year-to-year variability.

c. *Spatial distribution of the amplitude and frequency of CISO*

The largest standard deviation of CISO for the May–October season is found over the vast area of the western North Pacific centered at 15°–20°N, 140°–150°E (Fig. 3b). A secondary maximum is located over the Bay of Bengal. This is quite different from that of the base annual cycle. The latter exhibits maximum amplitude over Indian subcontinent with another weaker center over the Philippine Sea (Fig. 3a). Note also that the base annual cycle tends to concentrate in a relative narrow band along 10°–25°N, whereas significant CISO variability covers a broader latitude band from the equator to 30°N. The largest CISO variability is located between the western Pacific monsoon trough and subtropical ridge. The amplitude of CISO over Indochina peninsula is the minimum that separates ISM and WNPSM.

The primary oscillation period illustrated by the statistically most significant spectral peak also varies with locations (Fig. 4). Over Philippines and WNPSM region, 30 (25–35) day oscillation dominates, whereas

over ISM and EASM regions, the prevailing oscillation period is about 60 days.

3. Statistical significance of monsoon singularities

a. Statistical significance tests

As discussed in the introduction, the monsoon singularities are usually reflected by the extreme phases of CISO. Given the fact that the climatology is made from a limited sample size (17 yr in our OLR dataset), the statistical significance of the monsoon singularities must be tested. In what follows we carry out three types of local significance tests to identify monsoon singularities and to show that the climatological pentad mean departures associated with these singularities are unlikely insignificant residuals.

The first test is a sign test. The null hypothesis is that a negative (or positive) OLR anomaly occurs randomly at any given pentad of the calendar year, so that the probability of its occurrence is 50%. With this null hypothesis, it can be readily shown that at any given pentad the probability for more than 11 negative (or positive) anomalies to occur during the 17 summers (from pentad 25 to pentad 60, or 1 May–27 October) would be less than 5%. Therefore, if 12 or more wet (or dry) events occur at a specific pentad for the 17 summer sample, that pentad is referred to as a wet (or dry) singularity, corresponding to a 95% confidence level.

The second test (extreme test) is designed for testing the significance of the prominent maxima and/or minima of the OLR CISO. To be objective, we define, using ISO component of the pentad mean OLR series, $(\mathrm{OLR})_{\mathrm{ISO}}$, a prominent minimum as the one that satisfies the following criteria: (a) $(\mathrm{OLR})_{\mathrm{ISO}}$ is lower than -15 W m^{-2} and (b) $(\mathrm{OLR})_{\mathrm{ISO}}$ decreased more than 15 W m^{-2} from the previous peak and followed by a total increase exceeding 15 W m^{-2}. With the above definition, a total of 68 wet extrema are found during the 17 summers at 15°N and 140°E. That is to say, on average, there are four prominent OLR minima occurring in each summer. The averaged frequency of occurrence of a wet extreme in any given pentad is 1.9 (68/36). Under the null hypothesis that the wet extreme of CISO occurs randomly during the summer season, the probability density function for the frequency of occurrence of a wet extreme in a given pentad was determined using Monte Carlo simulation by performing total of 100 000 experiments. The observed statistics used in the simulation include the fact that the transient ISO has, on average, four prominent OLR minima per summer and any two adjacent minima must exceed three pentads. Otherwise, the wet extrema take place randomly. The resultant hypothetical probability distribution shown in Fig. 5 indicates that the probability for more than five (six) wet extrema to occur in a fixed calendar pentad during a 17 summer sample is less than 5% (1%). Taking a 95% confidence level, if six or more wet extrema occur in any given pentad, one should reject the null hypothesis, that is, the wet extreme singularity is statistically significant.

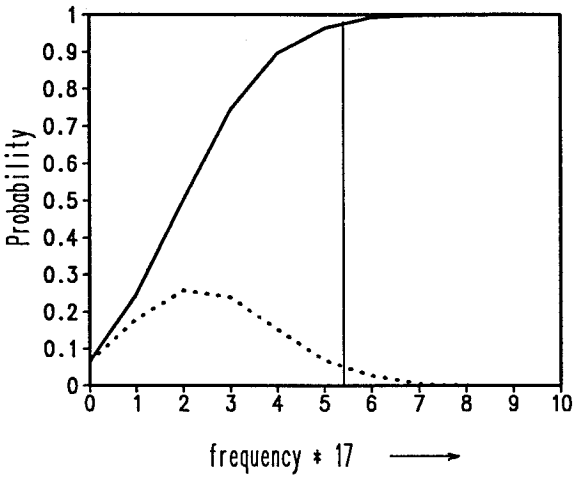

FIG. 5. The probability density function (dashed) and cumulative probability function (solid) for the frequency of occurrence of a prominent OLR minimum at any given calendar pentad determined by Monte Carlo simulations with 100 000 realizations. The thin solid lines indicate 95% cumulative probability.

The third test (*t*-test) examines the null hypothesis that the observed sample mean (the amplitude of CISO) at a fixed pentad has been drawn from a population characterized by zero mean, that is, the amplitude of CISO at a fixed pentad is not significantly different from zero. Assume n ($=17$) is the sample size, the test statistic,

$$t = A/(S/n^{1/2}), \tag{3.1}$$

follows a student's t distribution with the degree of freedom, $n - 1$, where A denotes the amplitude of CISO and S the sample standard deviation that results from the year-to-year variation. If $t > 2.12$ (for $n = 17$), i.e. A is more than about twice as large as the denominator (the standard deviation of the sampling distribution of the year-to-year departure), the null hypothesis would be rejected at the 95% confidence level, implying that the climatological pentad mean departure should not be viewed as an ordinary sampling fluctuation.

b. NH summer monsoon singularities

The statistically significant wet/dry singularities of CISO detected by the above three tests are shown in Fig. 6 for five selected locations in WNPSM, ISM, and Baiu. Obviously, significant singularities occur in association with the extremely wet or dry phases of CISO. For clarity, in this paper we define summer monsoon singularities by those extreme phases of CISO that pass at least two types (among the above three) of statistical tests at 95% confidence level. Monsoon singularities vary with locations. For instance, the most significant

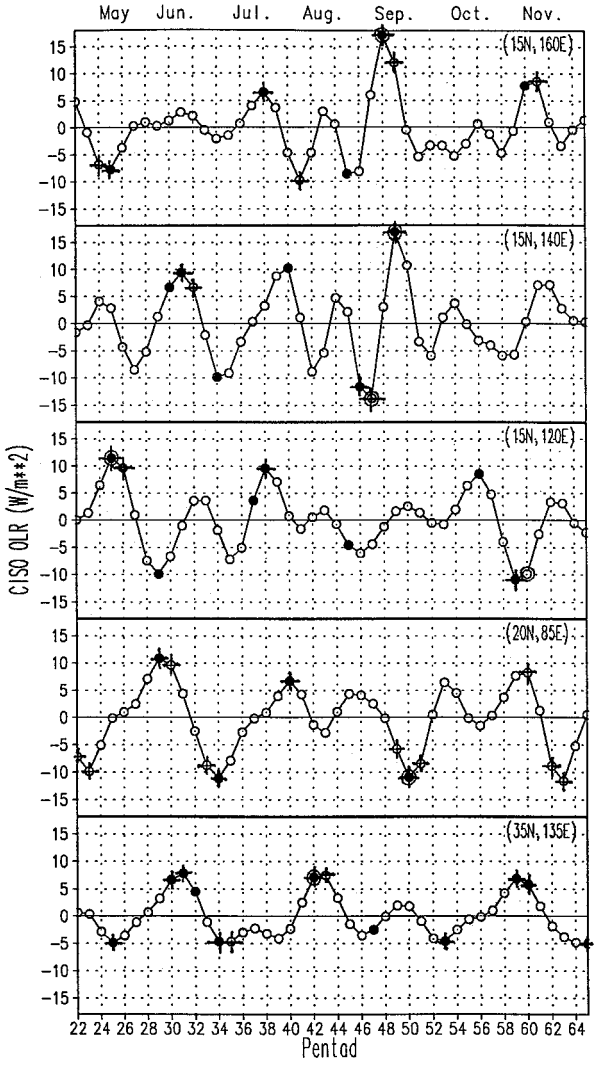

FIG. 6. OLR (in units W m^{-2}) CISO time series at selected 5° lat × 5° long boxes centered at (a) 15°N, 160°E (western North Pacific 1); (b) 15°N, 140°E (western North Pacific 2); (c) 15°N, 120°E (Philippines); (d) 20°N, 85°E (northeast India and Bay of Bengal); and (e) 35°N, 135°E (Japan). The locations of the five boxes are shown in Fig. 3a. Singularities that are statistically significant at 95% confidence level are detected by the sign-, extreme-, and *t* tests, which are marked out by solids, rings, and crosses, respectively.

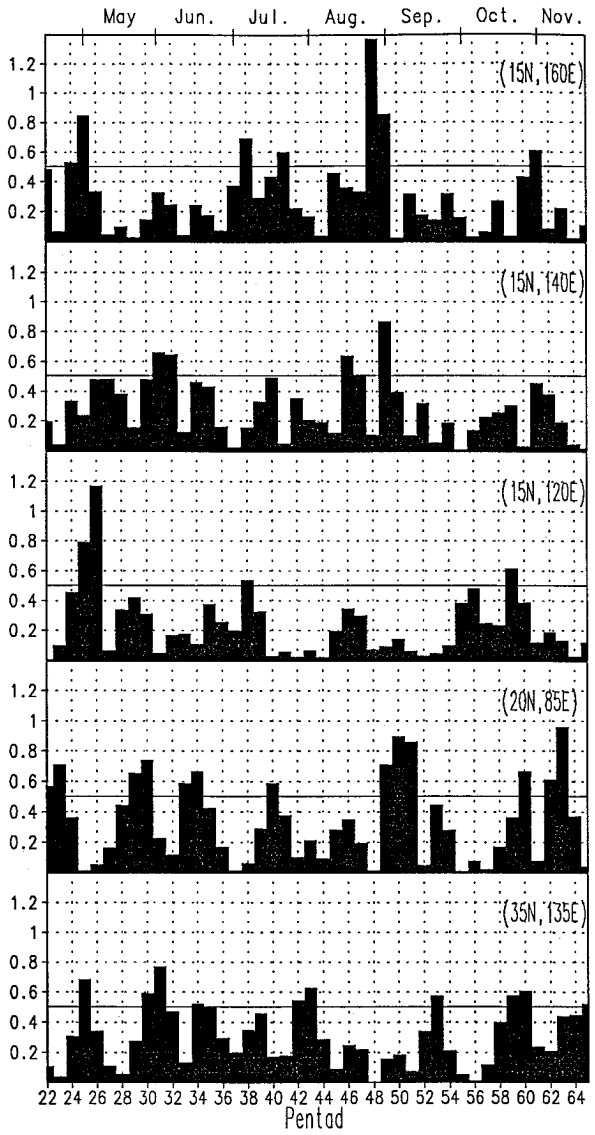

FIG. 7. Histograms showing the ratio *A*/*S* for each pentad from P22 to P65 and for five representative locations. Here *A* denotes the amplitude of CISO, whereas *S* represents the standard deviations of the ISO component which is associated with the year-to-year variation. The values higher than 0.51 indicate monsoon singularities detected by *t* test at 95% confidence level.

singularities are the peak monsoon and the ensuing break in the WNPSM (Figs. 6a,b); the pre-onset dry and the last wet spell over the South China Sea and Philippines (Fig. 6c); the pre-onset dry, the onset, and the wet spell in early September over the Bay of Bengal (Fig. 6d); and the pre-onset dry, the onset, and the midsummer dry after the Baiu over Japan (Fig. 6e).

The *t* statistic (3.1) also provides a measure of the relative magnitude of the CISO variability (*A*) with respect to the variability that is not phase locked to the annual cycle (*S*). Figure 7 shows the ratio *A*/*S* for each pentad from P22 to P65 and for the five selected locations shown in Fig. 6. A value of this ratio exceeding about 0.5 should trigger rejection of the null hypothesis and imply a statistically significant singularity. In general, the year-to-year variability is much larger than the CISO component in most pentads. However, for most statistically significant singularities, the amplitude of CISO (or the standard deviations of the phase-locked component of ISO) is comparable to the standard deviation of the non-phase-locked component of ISO. It is equally important to note the existence of the pentads in which the ratio *A*/*S* is close to zero, implying predominance of the year-to-year variability. These pentads correspond to transitional phases of CISO during which

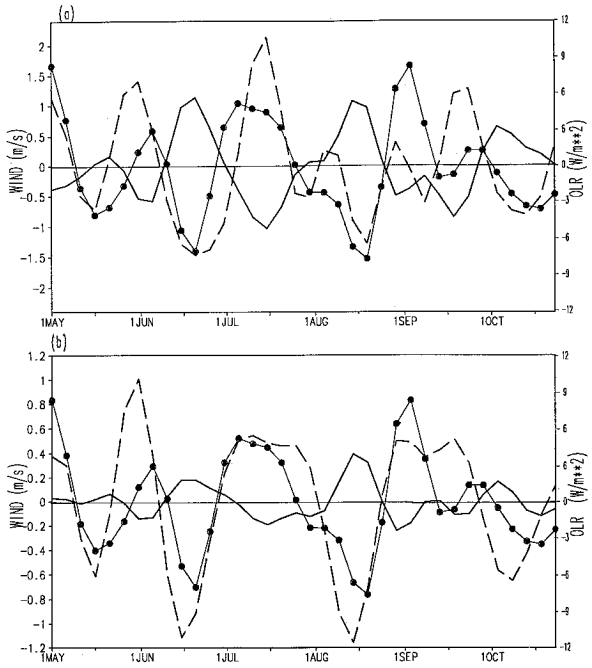

FIG. 8. The CISO index (the curve with solids) defined by the OLR CISO averaged over the Philippine Sea (10°–20°N, 120°–140°E) and the associated circulation anomalies: (a) the 850-hPa zonal wind anomaly (solid) averaged over (0°–15°N, 100°–140°E) and 200-hPa zonal wind anomalies (dashed) averaged over (5°S–10°N, 100°–150°E); (b) the cross-equatorial meridional wind anomaly at 850-hPa averaged over (5°S–5°N, 100°–135°E) (solid) and at 200 hPa averaged over (5°S–5°N, 95°E–140°E) (dashed).

the year-to-year variations are extremely prominent. These ''antisingularities'' are important for study of interannual variations of summer monsoons.

4. Dynamic structure of CISO

In the previous section we have shown the statistical significance of CISO and associated monsoon singularities. We will further examine, in this section, physical coherencies among the various meteorological fields associated with CISO. In particular, we derive CISO circulation anomalies from the ECMWF 850- and 200-hPa winds that are independent of OLR data. If CISO is a physically meaningful phenomenon (not a statistical artifact), one would expect that the OLR and wind anomalies associated with CISO exhibit dynamically coherent structure.

To test the dynamic consistency of CISO, we define a CISO index using the climatological pentad mean OLR anomalies averaged over the Philippine Sea (10°–20°N, 120°–140°E). The CISO index is shown in Figs. 8a and 8b. Based upon the theories of tropical atmosphere response to diabatic heating (Webster 1972; Gill 1980), one would expect Rossby wave response generating low-level westerlies and upper-level easterlies to the south and southwest of the heating. The climatological pentad mean 850-hPa zonal wind anomalies averaged over (0°–15°N, 100°–140°E) are indeed well negatively correlated (correlation coefficient is 0.8) with the index, whereas the 200-hPa zonal wind anomalies averaged over (5°S–10°N, 100°–150°E) are well positively correlated (correlation coefficient 0.6) with the Index (Fig. 8a). This implies that the enhanced convection over the Philippine Sea is certainly accompanied by enhanced low-level westerlies and the upper-level easterlies to its south and southwest. In view of the equatorial asymmetry of the heating depicted by the OLR index, one would also expect a response of cross-equatorial flow south of the heating. Figure 8b shows that in the lower troposphere, northward cross-equatorial winds between Sumatra and New Guinea (105°–135°E) are enhanced during the wet period (low index); meanwhile, the reversed upper-tropospheric cross-equatorial winds are greatly enhanced over the Maritime Continent. These cross-equatorial winds reflect variations in the local Hadley circulation associated with CISO. The high correlations between the OLR anomalies and ECMWF circulation anomalies indicate a robust dynamic consistence between two independent observations. This adds confidence to our analysis of CISO.

A mean structure of the CISO mode is reconstructed by regressing climatological pentad mean OLR and 850- and 200-hPa wind anomalies with the CISO index. Only statistically significant features are depicted in what follows with reference to Fig. 9. In the lower troposphere (850 hPa), strong cyclonic circulation is located about 10° longitude northwest of the convection anomaly. Prominent westerly anomalies extend from the Indian monsoon region eastward all the way to 145°E. In the upper troposphere (200 hPa), an anomalous anticyclone is located slightly to the west of the convection anomaly with intense easterly anomalies to the south and southwest of the convection. Note that the upper-level winds contain a notable divergent component that manifests itself as an exceptionally strong cross-equatorial northerly over the Maritime Continent.

The overall characteristic structure of the CISO is dominated by the lowest baroclinic vertical mode. The equatorial Rossby wave response causes horizontal asymmetry in winds: strong zonal wind anomalies are found to the south and southwest of the convection, but there are relatively weak zonal wind anomalies to the north and east. Vertically, low-level winds are dominantly rotational, whereas upper-level winds display a strong divergence and prominent cross-equatorial northerlies. The vertical asymmetry is caused by the effects of mean monsoon circulation. Similar structure for transient ISO was found and explained by Kawamura et al. (1997).

5. Propagation of CISO and the linkage among ISM, EASM, and WNPSM

The timing of monsoon singularities varies with locations as indicated in Fig. 6. The temporal phase re-

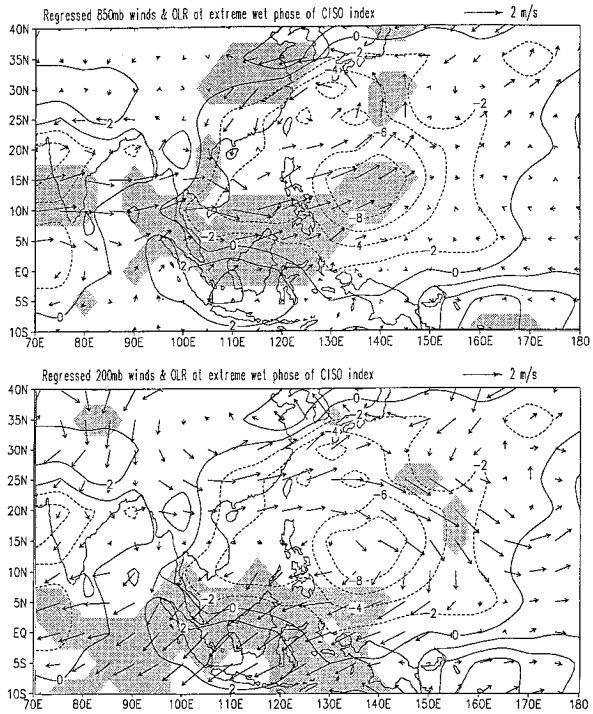

FIG. 9. The structure of the CISO derived by regressing pentad mean OLR and winds with the CISO index: (a) OLR and 850-hPa wind anomalies and (b) OLR and 200-hPa wind anomalies. The OLR index is shown in Fig. 8. The contours are regressed OLR anomalies (contour interval: 3 W m^{-2}). Areas in which wind anomalies are statistically significant at the level 95% are shaded.

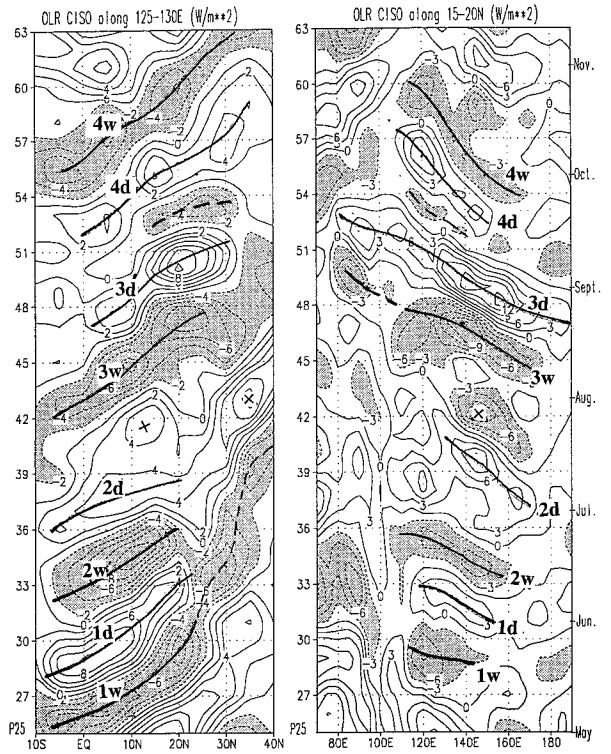

FIG. 10. Hovemoller diagrams of OLR CISO averaged along (a) a longitude band between 122.5° and 132.5°E and (b) a latitude band between 12.5° and 22.5°N. Four major propagation episodes are outlined by heavy lines and indicated by corresponding labels. Crosses indicate the quasi-standing episode occurring in between episodes 2d and 3w.

lationship among monsoon singularities at various locations can be investigated by examining the phase propagation of CISO. Figure 10 displays two Hovemoller diagrams of OLR CISO, one along the longitude band between 122.5° and 132.5°E (Fig. 10a) and the other along the latitude band between 12.5° and 22.5°N (Fig. 10b).

Along the longitude band 122.5°–132.5°E, the OLR CISO displays systematic northward phase propagation, which generally starts from south of the equator (5°S) and reaches 20°–30°N (Fig. 10a). There are four major episodes of northward propagation of convective anomalies from May to October as outlined by heavy solid curves and marked by 1w, 2w, 3w, and 4w. Each of the episodes endures about 30 days. The averaged northward propagation speed between the equator and 20°N is about 7° lat $pentad^{-1}$ or 1.8 m s^{-1}. From early May to mid-July northward propagation is systematic and almost ceaseless from 5°S to 20°N. This reflects the characteristics of the tropical monsoon to the south of western Pacific high. Beyond 25°N, the northward propagation is much slower, indicating change of propagation character in the subtropical monsoon (Meiyu/Baiu) region. The northward propagation along other longitude bands from 60°E to 170°W are also examined. The most evident northward propagation, however, is found between 110° and 130°E. The signals over other longitude bands are weak.

Along the latitude band between 12.5° and 22.5°N, CISO exhibits a pronounced westward propagation primarily over the western Pacific between 110° and 160°E (Fig. 10b). The zonal extent of the westward propagation enlarges with seasonal march from June to August and shrinks afterward. In the strongest episode, occurring from early August to mid-September, the convective anomalies propagate all the way from the dateline to the South China Sea (110°E) or the Bay of Bengal (80°E). The averaged westward propagation speed is 15–20 degrees of longitude per pentad or 4–5 m s^{-1}.

The phase relationship of ISO among ISM, EASM, and WNPSM regions has been controversial. Nakazawa (1992) noticed two active phases of intraseasonal variability that appear to link ISM and Baiu. One occurs in late May and early June over the Indian Ocean concurrent with the onset of South India and south Japan monsoons. The other takes place in late July over the western Pacific and terminates Baiu and activates monsoon over the Indian Ocean. On the other hand, J. Matsumoto and T. Murakami (1995, personal communication) emphasized the close linkage of intraseasonal monsoon variability between WNPSM and Baiu. The link-

age between the EASM and the tropical monsoons (ISM and WNPSM) has also been extensively studied but remains an unresolved issue (Zhu 1988; Zeng et al. 1994).

The predominant movement of CISO has direct implications on the relationship among the mean evolutions of WNPSM, ISM, and EASM. The first episode of northward propagation shown in Fig. 10a implies a link between the onset of the tropical monsoon (SCSPSM) at P28 and subsequent onset of subtropical monsoon, Meiyu/Baiu at P32–P33. The onset of Meiyu/Baiu is characterized by a sudden shift of convective anomalies from about 23°N to 29°N from P32 to P34, which is nearly in phase with the onset of WNPSM. During that period, the WNPSM trough, Western Pacific High, and EASM trough form an interactive dynamic system: the enhancement of WNPSM concurs with the sudden change of position or intensity of the Western Pacific High, which in turn induces sudden shift of the rain belt in EASM. The coupling between the variability of WNPSM trough and that of Western Pacific High, however, becomes weak after the Meiyu/Baiu season. We will further elaborate this point in section 7.

Regarding the relationship between ISM and WNPSM, the result in Fig. 10b indicates that the phase propagation and the oscillation period over the Bay of Bengal differs from those over the western North Pacific. This, however, does not mean they are not related. In fact, there is a tendency of out-of-phase relationship between ISM and WNPSM convection. During August and September, when the extent and strength of the westward propagation of CISO are strongest, slow westward propagation of CISO makes the convective variation in ISM roughly out of phase with that in WNPSM (Fig. 10b). From mid-June to late July, on the other hand, ISM and WNPSM evolve nearly in-phase. This results from a nearly in-phase northward propagation of zonally oriented CISO anomalies in both the Indian and western Pacific sectors as will be shown in the next section. The correlation in OLR anomalies between ISM and WNPSM averaged over entire summer season is rather unstable. This is, to some extent, consistent with previous studies that found that the western North Pacific convection inversely related to the equatorial Indian Ocean convection on the 30–60-day timescales [the EOF 1 of Lau and Chan (1985) and Zhu and Wang (1993), but the link between WNPSM and ISM convection appears to be weak, see EOF 1 and EOF 2 pattern of Lau and Chan (1986)]. We emphasize that the relationship between WNPSM and ISM varies with seasonal march. Any blended analysis for the entire summer season would result in a weak correlation.

6. CISO cycles linking Northern Hemisphere summer monsoon singularities

The movement of CISO is two-dimensional. Northward and westward propagation tend to occur in tandem

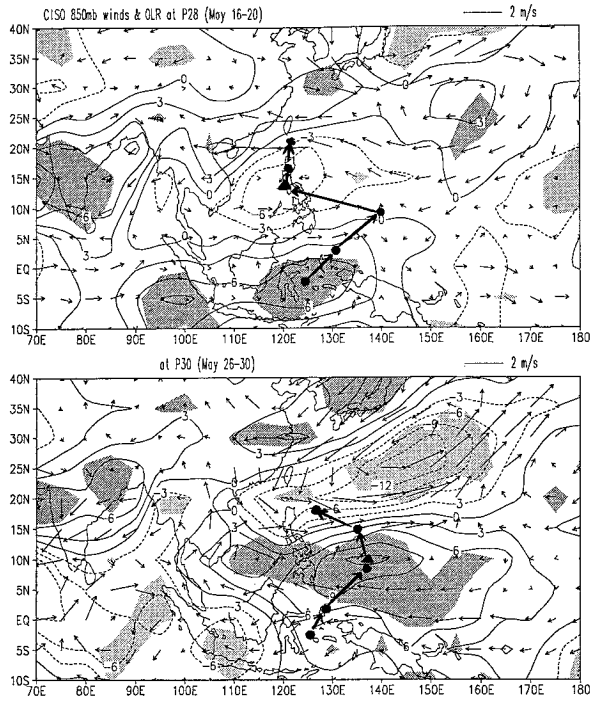

FIG. 11. The extremely wet (P28) (a) and dry (P30) (b) phases of CISO Cycle I. Contours show OLR anomalies at an interval of 3 W m^{-2} and arrows show anomalous 850-hPa winds. Heavy (light) shadings denote, respectively, areas with statistically significant wet (dry) singularity at 95% confidence level. The heavy triangle indicates the center of OLR anomalies at the extremely wet or dry phases. Heavy solids along with the arrows indicate the tracks of the OLR anomaly centers on consecutive pentad maps.

(Fig. 10). However, in May and June when northward propagation is prominent along 122.5°–132.5°E, the westward propagation is ill defined. On the other hand, from mid-July to mid-September, northward propagation is relatively weak, whereas the westward propagation along 15°–20°N is very strong.

In order to better depict two-dimensional movement and development of CISO, pentad mean OLR CISO maps from May to November are used to analyze its evolution. In each pentad mean map, the area where locally significant (LS) wet or dry phase at the 95% confidence level are shaded. The significance of a pattern can be judged by first calculating the percentage of the field in a given pentad that is locally significant and then determining the probability that this percentage would be observed randomly (Livezey and Chen 1983). A pattern is significant if the pattern contains LS areas exceeding a critical percentage of the total domain for given degree of freedom (grid points in the domain). The pattern significant tests that are performed for each pentad mean map shown in Figs. 11–14 and for OLR and 850- and 200-hPa winds indicate that the principal systems associated with CISO are statistically significant.

Based on climatological pentad mean anomaly maps,

TABLE 1. Summary of the four major CISO cycles and NH summer monsoon singularities. The monsoon singularities that pass two or more statistical tests (one test) are written in upper- (lower-) case letters. The onset and end of monsoon rainy season are also marked with letters in brackets. Symbols in the column ''jump'' represent the direction and distance of the sudden jump of CISO OLR anomaly centers. For instance, N10 denotes a sudden northward shift by 10°.

PEN-TAD	Date	OLR CISO			Monsoon singularities			
		''jump''	cycle		15°N, 120°E	15°N, 140°E	35°N, 135°E	20°N, 85°E
26	5/6–10				DRY			
27	11–15				DRY			
28	16–20	N 5, W 20	I	W1	(onset)			
29	21–25				active			DRY
30	26–30	N 5		D1		dry	DRY	dry
31	5/31–6/4					DRY	DRY	
32	6/5–9					dry	dry	(onset)
33	10–14					(onset)	(onset)	active
34	15–19	N 10		W2		active	ACTIVE	ACTIVE
35	20–24				active		active	
36	25–29		II					
37	6/30–7/4						PEAK	
38	7/5–9	N 10			BREAK			
39	10–14			D2				
40	15–19					break		BREAK
41	20–24						(end)	
42	25–29	N 10					DRY	
43	7/30–8/3						DRY	
44	8/4–8							
45	9–13	W 15			active			
46	14–18			W3		ACTIVE		(break)
47	19–23					ACTIVE	wet	
48	8/24–28		III					
49	29–9/2					BREAK		active
50	9/3–7	W 15		D3	break			ACTIVE
51	8–12							active
52	13–17							
53	18–22						wet	
54	23–27							
55	9/28–10/2			D4		(break)		
56	10/3–7				break			(active)
57	8–12		IV					
58	13–17			W4		(active)		(end)
59	18–22	NW 10			ACTIVE		DRY	
60	23–27				ACTIVE	(end)	DRY	
61	10/28–11/1	N 5			(end)			

we identify four major CISO cycles during the northern summer that link major climatic singularities in the NH summer monsoons. They are summarized in Table 1 and implemented by the following description. The monsoon singularities are marked for four selected locations that represent WNPSM (15°N, 140°E), Meiyu/Baiu (35°N, 135°E), ISM (20°N, 85°E), and the South China Sea–Philippines summer monsoon (SCS–PSM) (20°N, 120°E), respectively. The latter is special in the sense that the area of the South China Sea and the Philippines joins three major monsoon areas. It is located in a low-level confluence zone where the southwesterly from India, the cross-equatorial southerly from the Southern Hemisphere, and the easterly from the North Pacific converge.

a. Cycle I (prelude cycle): P26–P31 (6 May–4 June)

This is a period prior to the onsets of ISM, WNPSM, and Meiyu/Baiu. During this cycle, however, the summer monsoon first starts over the South China Sea and the Philippines. Before the onset in early May, the vast area of southeast Asia and the tropical western North Pacific is covered by positive OLR anomalies with a center over the Philippines, corresponding to a pre-onset dry singularity of the South China Sea–Philippine summer monsoon (SCS–PSM) (Fig. 6c). From P27 to P28 (May 16–20) the negative OLR anomaly center suddenly shifts northwestward; the original dry area is replaced by negative OLR (convective) anomalies and associated low-level cyclonic circulation anomalies, which then rapidly intensify, establishing a wet singularity near the northern Philippines and significant low-level westerly anomalies (2 m s^{-1}) over the South China Sea (Fig. 11a).

The convective anomalies are primarily originated from the equatorial ocean between Borneo and New Guinea and take a zigzag northward track as illustrated in Fig. 11a. This is also consistent with the northward propagation of negative OLR band 1w shown in Fig.

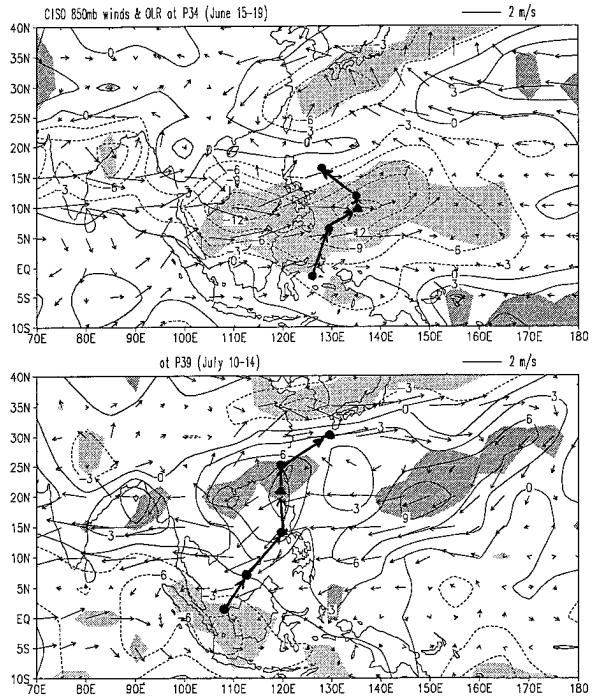

FIG. 12. As in Fig. 11 except for CISO Cycle II with an extremely wet (dry) phase at P34 (P39).

10a. The rapid northward movement of convective anomalies is also an indication of the sudden shift of monsoon trough from the equatorial region to about 10°N along 120°–130°E. In tandem with the northward shift of the western Pacific monsoon trough, the east Asian subtropical monsoon front develops over the southeast coast of China, Taiwan, and Okinawa, starting rainy seasons there (Tanaka 1992).

The peak dry phase of Cycle I (P30) is characterized by a belt of intense positive OLR (dry) and low-level anticyclonic anomalies extending from Malaysia all the way eastward to the dateline between 5° and 20°N (Fig. 11b). This dry phase represents premonsoon dry singularities of the WNPSM, ISM, and Meiyu/Baiu. The dry zone was originated from the equatorial maritime continent at P28 and moved northward continuously as shown by the positive OLR band 1d on Fig. 10a.

b. Cycle II (Onset cycle): P32–P40 (5 June–19 July)

After the premonsoon dry period, the WNPSM, ISM, and Meiyu/Baiu begin during the wet phase of Cycle II (5–14 June) (Figs. 6b,d,e and Table 1). The onsets determined from CISO activity agree with the results of previous analyses based on rainfall data (e.g., Rao 1976; Tao and Chen 1987; Tanaka 1992; Murakami and Matsumoto 1994). The wet phase of the Cycle II reaches peak at P34 (15–19 June) after a sudden northward jump of the convective anomaly over the western Pacific (Fig. 12a). All three monsoons experience simultaneously active monsoon rain after their onsets. Cyclonic circulation anomalies accompany convective anomalies with enhanced westerlies over the tropical monsoon domain between 5° and 20°N and extending from Indian subcontinent all the way to 150°E.

The dry phase of Cycle II starts at P36 and reaches a crest around P39 (10–14 July) after the giant dry anomaly suddenly ''jumped'' from 10°–15°N to 20°N at P38 (Fig. 12b). All major summer monsoons, including ISM, WNPSM, and SCS–PSM, undergo an in-phase break—a grand break period (Table 1). At the same time, the short lifespan Meiyu over the middle and lower reaches of the Yangtze river and the Baiu in southern Japan cease. The enormously large dry areas coincide with an anomalous low-level anticyclone with notable easterly anomalies prevailing in the entire tropical southeast Asia and western North pacific (Fig. 12b). The EASM rain belt advances from the Yangtze river valley northward to the Yellow river valley and northern Korea peninsula.

A prominent feature of Cycle II is the nearly in-phase evolutions between ISM and WNPSM, as well as the Meiyu/Baiu. Both the enhanced and suppressed convection during the wet and dry phases of this cycle display east–west oriented giant band structures that move dominantly northward as indicated by the central tracks of the wet and dry anomalies in Fig. 12 and the negative and positive OLR anomaly bands 2w and 2d on the Hovemoller diagram Fig. 10a. The convective anomalies are formed at P32 over Sulawesi Sea. From P32 to P34 the convective anomalies rapidly reintensify and suddenly shift northward by about 10 degrees of latitude. The northward movement continues until P36. The suppressed convection areas occur first over the equatorial region from the central Indian Ocean to Borneo and then move northward to about 25°N from P36 to P40.

c. Cycle III (peak cycle): P44–P52 (4 August–17 September)

In between Cycle II and Cycle III, from P41 to P43 (20 July–3 August), there is a regional monsoon singularity primarily over the Northwestern Pacific. It was a main theme of the discussions in the papers of Nakazawa (1992) and Ueda et al. (1995). In late July (P42), large-scale convective activity abruptly develops in a region centered at 20°N and 150°E. The Western Pacific High exhibits a simultaneous northward jump to its northmost position, controlling Japan, Korea, the Yellow Sea, and the Shandong peninsula of China, bringing midsummer hot weather there and pushing EASM rain belt farther north to northeast China (north of 40°N). At the same time, the development of tropical cyclones in the region of 15°–25°N and 140°–150°E suddenly enhanced and the tropical storm tracks change pattern (Kawamura et al. 1994). In Fig. 10, this abrupt episode was

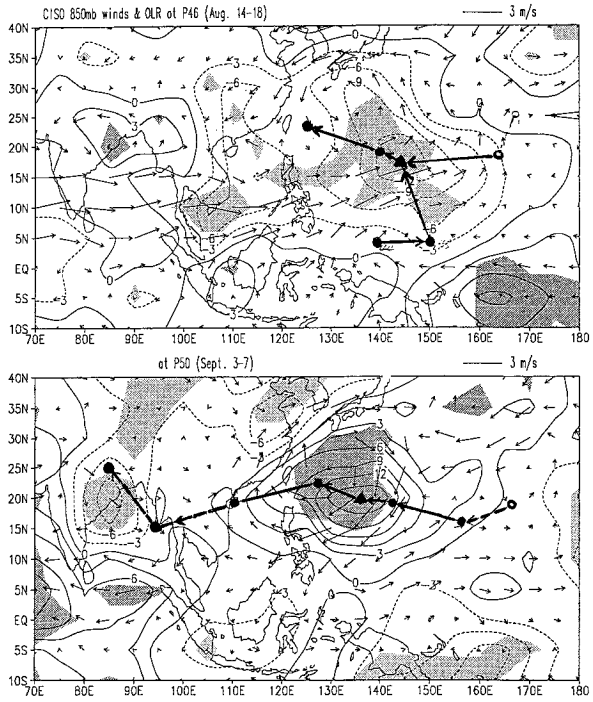

FIG. 13. As in Fig. 11 except for CISO Cycle III with an extremely wet (dry) phase at P46 (P50).

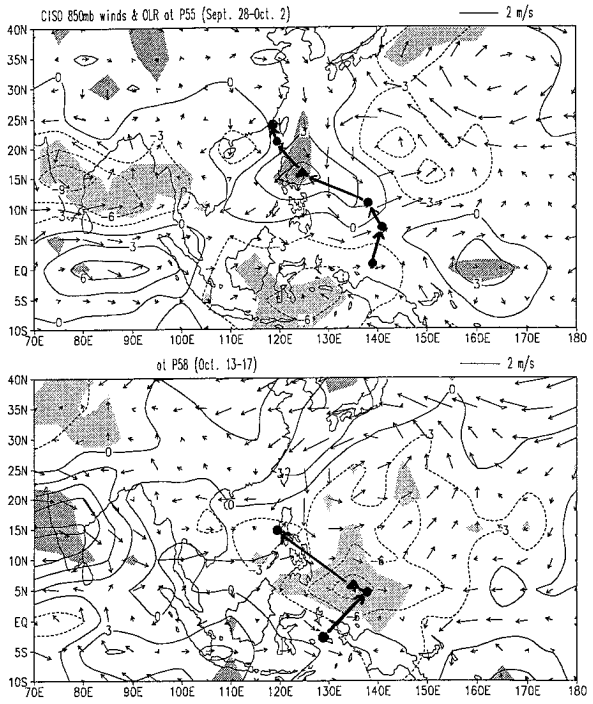

FIG. 14. As in Fig. 11 except for CISO Cycle IV with an extremely dry (wet) phase at P55 (P58).

marked out by heavy crosses. It is a standing event and confined to the northwestern Pacific.

The wet phase of Cycle III starts at P44 (4–8 August) and peaks around P46 (14–18 August). The initial convective and low-level cyclonic anomalies develop at two regions: one is north of Sulawesi–New Guinea and the other near the dateline around 25°N, 170°E. The former moves northward and the latter moves westward, leading to a merge and abrupt intensification at P46 (Fig. 13a). After P46 the convective anomaly migrates westward, reaching Taiwan by P48. The described movement is clearly shown by the negative OLR band 3w in Figs. 10a and 10b. Pentad 46 (14–18 August) benchmarks the peak phase of WNPSM and SCS–PSM (Figs. 6a–c, Table 1). The western Pacific monsoon trough reaches its northmost position as evidenced by strong westerly monsoon anomaly penetrating eastward to 160°E. Meanwhile, the Western Pacific High weakens as indicated by the cyclonic circulation anomaly centered at 25°N, 140°E.

The peak WNPSM is followed by a second major break (Figs. 6a–c, Table 1), which is associated with the most prominent westward propagation of the large-scale suppressed convection in the dry phase of Cycle III. The westward propagation is primarily along 15°–20°N and from the dateline at P47 to the Bay of Bengal at P52, in good agreement with the positive OLR band 3d shown in Fig. 10b. The peak dry phase of the Cycle III at P50 is characterized by an anomalously strong western Pacific subtropical high south of Japan as revealed by the strong anomalous anticyclone and extremely large positive OLR anomaly (Fig. 13b). At the same time, the EASM rain belt retreats back to the Yellow River and Yangtze River valleys and Japan experiences an autumn rainy season (Shurin). In contrast to the WNPSM region, the ISM region is dominated by strong convective anomalies at P50, which reflects active monsoon in northeast India and the Bay of Bengal. Northeast India and the Bay of Bengal experience the second major break around P53 upon the arrival of the westward migrating dry anomalies of the Cycle III (Fig. 10b). During Cycle III, the OLR variations in ISM and WNPSM are completely out of phase.

d. Cycle IV (withdrawal cycle): P53–P61 (18 September–1 November)

After the dry anomalies of Cycle III decayed, there is a very weak and brief wet period from P53 to P54 as shown by the dashed heavy lines in Figs. 10a and 10b. From P54 a new cycle starts with a dry phase peaking at P55 (29 September–2 October) (Fig. 14a) and a wet phase peaking at P58 (13–17 October) (Fig. 14b). Two notable features are observed. First, whereas westward propagation remains evident (heavy lines 4d and 4w in Fig. 10b), both the dry and wet anomalies migrate predominantly northward as shown by the central tracks in Fig. 14 and the heavy lines 4d and 4w in Fig 10a. Second, there is a nearly 180° out-of-phase relationship in convective activity between ISM and

WNPSM. In addition, the contrast between dry and wet phases of Cycle IV is not as distinct as the previous three cycles. The most significant monsoon singularities are observed in SCS–PSM region (Fig. 6c). The wet phase of Cycle IV from P57 to P59 represents the last wet spell of WNPSM and SCS–PSM. The monsoon over central and northeast India, on the other hand, retreats during the same period (Rao 1976). The WNPSM withdraws at P61 after the last wet spell (Fig. 6b).

7. Summary

a. Conclusions

We have presented evidences that the transient intraseasonal oscillations (ISOs) in the NH summer monsoon domain, especially in the western North Pacific, tend to be phase locked to annual march of planetary-scale monsoon circulation. The phase-locking results in a *climatological intraseasonal oscillation* (CISO), which appears to be significant at 95% confidence level in terms of three different types of statistical test. The extreme phases of CISO characterize summer monsoon singularities. In the context of weather and climate, singularity is an event that occurs on or near a fixed date with usual regularity.

The concept of *summer monsoon singularity* is important and useful for describing and understanding temporal structures of monsoon climate and variability. Whereas monsoon singularities depict those events that have remarkable regularity, the occasional breakdown or debasement of the regularity implies a robust signal of interannual variation. More importantly, *transitional phases* of CISO, in contrast to extreme phases, indicate the periods during which summer monsoons experience largest year-to-year variability. Since a strong or weak monsoon season is often linked to changes in the duration and intensity of major active/break monsoons, study of monsoon singularity may provide useful information for understanding and predicting monsoon variability.

The CISO exhibits a coherent dynamic structure between convective and circulation anomalies (Fig. 9). Enhanced convection is located to the southeast of 850-hPa positive vorticity center and in phase with 200-hPa divergence anomalies. Both enhanced 850-hPa westerlies and 200-hPa northeasterlies are located to the southwest of the enhanced convection. The upper-level winds contain a significant divergent component that manifests itself as an exceptionally strong cross-equatorial northerly over the Maritime Continent. The low-level cross-equatorial southerlies are enhanced during the period of enhanced convection occurring in the western North Pacific, but their strength is relatively weak.

The CISO propagates. Although the movement is two-dimensional, there exist season-dependent, preferred patterns. Northward propagation dominates during early summer (May–July), whereas westward propagation prevails in August and September (Fig. 10). Most significant northward propagation is found along the Philippine Maritime Continent. The averaged northward propagation speed is about 1.8 m s^{-1}. Strongest signal of westward propagation occurs along 15°N–20°N and from 160° to 110°E with a typical speed of about 4–5 m s^{-1}. The movement of CISO links characteristic evolution of the monsoons in one region with those of neighboring areas.

Extreme phases of CISO often benchmark summer monsoon singularities (Fig. 6). Four major CISO cycles are identified from May to October (see Table 1). The peak wet phase of the first cycle at P28 (16–20 May) marks the onset of the South China Sea–Philippine summer monsoon (Fig. 11). It is followed by an extremely dry phase at P30–P31 (26 May–4 June) that corresponds to the premonsoon dry period over Indian Summer Monsoon (ISM), WNPSM, and Meiyu/Baiu regions. The wet phase of Cycle II peaking at P34 (15–19 June) represents the first wet spell after the grand onsets of ISM, WNPSM, and Meiyu/Baiu (Fig. 12). The crest of the dry phase of Cycle II at P39 (10–14 July) concurs with a grand break of ISM and WNPSM and the retreat of Meiyu/Baiu. The extremely wet phase of Cycle III at P46 (14–18 August) benchmarks the height of WNPSM (Fig. 13). The dry phase of Cycle III exhibits a prominent westward propagation from the dateline at P47 (19–23 August) all the way to the Bay of Bengal at P53 (18–22 September), which is responsible for the second break of WNPSM and ISM. The wet phase of Cycle IV in mid-October brings the last active monsoon in WNPSM and terminates ISM (Fig. 14).

The relationship in subseasonal variability between ISM and WNPSM varies with seasonal march. During the onset cycle (Cycle II), the evolution of ISM and WNPSM tends to be in phase due to the northward migration of east–west elongated CISO anomalies. On the other hand, during the peak cycle (Cycle III), the evolution of ISM is nearly 180° out of phase with WNPSM due to slow westward propagation of an east–west dipole CISO anomaly. During the first and the last cycle, however, they tend to evolve independently (Fig. 10b). The intraseasonal monsoon variations of EASM link more intimately with WNPSM than with ISM. This is due to the coupling among the WNPSM trough, the Western Pacific High, and the EASM trough. The coupling between the WNPSM trough and Western Pacific High, however, is also season dependent. During the first half of summer (early June to mid-July), evolution of WNPSM and EASM (Meiyu/Baiu) are nearly in phase due to a strong coupling between the WNPSM trough and Western Pacific High. In contrast, from late July to the end of August, the linkage between WNPSM and EASM is very weak due to (a) relatively independent evolution of the Western Pacific High and WNPSM trough and (b) dominant westward propagation of CISO anomalies during cycle III.

b. Discussion

What physical processes cause the phase locking of transient ISO to an annual cycle? We speculate that regulation of planetary-scale circulation change on movements of ISOs may play a critical role. The following discussions are focused on the most prominent CISO movements that are associated with the onset and peak cycles (the Cycle II and Cycle III).

The onset is associated with the wet phase of Cycle II of CISO during which enhanced convection originates from Maritime Continent and moves northward to about 20°N. It is initially associated with westerly anomalies to the south of an equatorial anticyclone (Buffer Zone) that moves northward, causing sudden onset of WNPSM in middle June. The prevailing northward propagation of CISO during early summer is favored by the seasonal march of planetary-scale circulation systems, in particular, the South Asia High and Western Pacific High. The northward movement of OLR CISO displays a close association with the ''stepwise'' displacement of the Western Pacific High. Note also that the northward propagation is most significant along the Philippine Maritime Continent. The island surface sensible heat flux may contribute to local rising temperature and dropping pressure and thus favors northward shift of the equatorial convergence zone. Yanai and Li (1994) emphasized the importance of sensible heating over the Tibetan Plateau in reversing meridional temperature gradient and the onset of ISM. The thermal effect of the Maritime Continent over the Philippines may function in a similar manner. The preferred northward propagation region is also a confluence zone between ISM southwesterly, cross-equatorial southerly, and WNP southeasterly. The role of the establishment of background low-level southerlies in ''steering'' convection anomalies northward should not be ruled out.

The WNPSM peak singularity is associated with the wet phase of CISO Cycle III, during which convective anomalies are originated around 170°E at P44 (4–8 August) and predominantly propagate westward along 15°–20°N (Fig. 10b and Fig. 3a), resulting in the height of WNPSM rainfall in middle August. The convective anomalies appear to be initiated in a region where the upper-level divergence associated with tropical upper-tropospheric trough (TUTT) nearly coincides with low-level convergence at the eastern end of the western Pacific monsoon trough. Previous studies have noticed the association of the convection in tropical Pacific with the TUTT (Sadler et al. 1976; Liebmann and Hartmann 1984; Chen and Yen 1991) and the convergence zone between monsoon westerlies and trades (Holland 1995). In August, the easterly vertical shear extends from south Asia all the way eastward to 170°E. The area of warmest SSTs expands to its northeast-most location in the western Pacific. Wang and Xie (1996) has shown that easterly vertical shear tends to strongly confine Rossby waves to the lower troposphere, which leads to enhanced boundary layer frictional moisture convergence and convective heating feedback. In addition, the easterly shear also enhances baroclinic conversion of mean available potential energy to equatorial Rossby waves (Xie and Wang 1996). The combined heating and baroclinic processes can effectively destabilize moist equatorial Rossby waves that move westward slowly. During the midsummer, the northmost position of the Western Pacific High and WNPSM trough provide a favorable environment for the development of westward propagating Rossby waves. The phase lock of Rossby wave activity with the peak of WNPSM circulation is very likely responsible for westward propagation of CISO during Cycle III.

The largest amplitude of CISO is found over the western North Pacific summer monsoon (WNPSM) region between the mean summer monsoon trough and the ridge of the Western Pacific High. The dominant period of CISO is about 20–30 days there. The WNPSM, therefore, features the most pronounced CISO and monsoon singularities. This appears to be due to 1) the impacts of subseasonal variability of the Western Pacific High and 2) the annual regulation of transient activity of slowly westward propagating wave disturbances in the western North Pacific as described by Murakami (1980), Chen and Xie (1988), and Wang and Rui (1990).

The strong activity of CISO and monsoon singularities over east Asia and the western North Pacific is one of the prominent characteristics of the boreal summer general circulation. Similar phenomenon was found significant in Austral summer monsoons in Indonesia and northern Australia. It bears profound implications to seasonal climate predictions. The present study provides a new perspective and framework for study of summer monsoon singularities, yet much more work is required to further understand dynamics of CISO and monsoon singularities, in particular, the precise dynamic processes that control the phase locking of ISO to seasonal march. This appears to be a result of complex nonlinear interaction between atmosphere, ocean, and land.

Acknowledgments. The authors are grateful for reviewers' comments, which resulted in an improved version of the manuscript. This study has been supported by the Climate Dynamics Program of the National Science Foundation under Grant ATM-94-00759 and the Marine Meteorology Program of Office of Naval Research. This is the School of Ocean and Earth Science and Technology Publication No. 4192.

REFERENCES

Chen, L.-X., and Z. Jin, 1984: The medium-range variations of the summer monsoon circulation system over east Asia. *Adv. Atmos. Sci.,* **2,** 124–233.

——, and A. Xie, 1988: Westward propagating low-frequency oscillation and its teleconnections in the eastern hemisphere. *Acta Meteorol. Sin.,* **2,** 300–312.

Chen, T.-C., and M. Murakami, 1988: The 30–50-day variation of

convective activity over the western Pacific Ocean with the emphasis on the northwestern region. *Mon. Wea. Rev.,* **116,** 892–906.

——, and M. C. Yen, 1991: Interaction between intraseasonal oscillations of the midlatitude flow and tropical convection during 1979 northern summer: The Pacific Ocean. *J. Climate,* **4,** 653–671.

Ding, Y.-H., 1992: Summer monsoon rainfall in China. *J. Meteor. Soc. Japan,* **70,** 373–396.

Gill, A. E., 1980: Some simple solutions for heat induced tropical circulation. *Quart. J. Roy. Meteor Soc.,* **106,** 447–463.

Hartmann, D. L., M. L. Michelson, and S. A. Klein, 1992: Seasonal variations of tropical intraseasonal oscillations: A 20–25-day oscillation in the western Pacific. *J. Atmos. Sci.,* **49,** 1277–1289.

Hendon, H., and B. Liebmann, 1990: The intraseasonal (30–50-day) oscillation of the Australian summer monsoon. *J. Atmos. Sci.,* **47,** 2909–2923.

Holland, G. J., 1986: Interannual variability of the Australian monsoon at Darwin: 1952–1982. *Mon. Wea. Rev.,* **114,** 594–604.

——, 1995: Scale interaction in the western Pacific monsoon. *Meteor. Atmos. Phys.,* **56,** 57–79.

Huang, R. H., 1994: Interactions between the 30–60-day oscillation, the Walker circulation and the convective activities in the tropical western Pacific and their relations to the interannual oscillation. *Adv. Atmos. Sci.,* **11,** 367–384.

Kawamura, R., T. Yasunari, and H. Ueda, 1994: Abrupt changes of seasonal evolution of large-scale convective activity and tropical cyclone over the western Pacific (in Japanese). *Rep. Nat. Res. Institute for Earth Science and Disaster Prevention,* **53,** 1–18.

——, T. Murakami, and B. Wang, 1997: Tropical and midlatitude 45-day perturbations during the northern summer. *J. Meteor. Soc. Japan.*, in press

Krishnamurti, T. N., 1985: Summer monsoon experiment—A review. *Mon. Wea. Rev.,* **113,** 1590–1626.

——, and H. N. Bhalme, 1976: Oscillations of a monsoon system. Part I. Observational aspects. *J. Atmos. Sci.,* **33,** 1937–1954.

——, and D. Subrahmanyan, 1982: The 30–50-day mode at 850 mb during MONEX. *J. Atmos. Sci.,* **39,** 2088–2095.

Lau, K.-M., and P. H. Chan, 1986: Aspects of 40–50-day oscillation during the northern summer as inferred from outgoing longwave radiation. *Mon. Wea. Rev.,* **114,** 1354–1367.

Liebmann, B., and D. L. Hartmann, 1984: An observational study of tropical–midlatitude interaction on intraseasonal timescales during winter. *J. Atmos. Sci.,* **41,** 3333–3350.

Livezey, R. E., and W. Y. Chen, 1983: Statistical field significance and its determination by Monte Carlo techniques. *Mon. Wea. Rev.,* **111,** 46–59.

Madden, R. A., 1986: Seasonal variations of the 40–50-day oscillation in the tropics. *J. Atmos. Sci.,* **43,** 3138–3158.

Matsumoto, J., 1992: The seasonal changes in Asian and Australian monsoon regions. *J. Meteor. Soc. Japan,* **70,** 257–273.

McBride, J. L., 1987: The Australian summer monsoon. *Monsoon Meteorology,* C. P. Chang and T. N. Krishnamurti, Eds., Oxford University Press, 203–231.

Murakami, T., 1980: Temporal variation of satellite-observed outgoing longwave radiation. Part I: Long-period (15–30-day) observations. *Mon. Wea. Rev.,* **108,** 408–426.

——, and J. Matsumoto, 1994: Summer monsoon over the Asian continent and the western North Pacific. *J. Meteor. Soc. Japan,* **72,** 719–745.

——, L.-X. Chen, and A. Xie, 1986: Relationship among seasonal cycle, low-frequency oscillation, and transient disturbances as revealed from outgoing longwave radiation data. *Mon. Wea. Rev.,* **114,** 1456–1465.

Nakazawa, T., 1992: Seasonal phase lock of intraseasonal variation during the Asian summer monsoon. *J. Meteor. Soc. Japan,* **70,** 597–611.

Ninomiya, K., and T. Murakami, 1987: The early summer rainy season (Baiu) over Japan. *Monsoon Meteorology,* C.-P. Chang and T. N. Krishnamurti, Eds., Oxford University Press, 93–121.

Rao, Y. P., 1976: Southwest monsoon. *Synoptic Meteorology,* Meteor. Monogr., No. 1/1976, India Meteor. Dept., 367 pp.

Sadler, J. C., 1976: A role of the tropical upper tropospheric trough in early season typhoon development. *Mon. Wea. Rev.,* **104,** 1266–1278.

Sikka, D. R., and S. Gadgel, 1980: On the maximum cloud zone and ITCZ over Indian longitudes during the southwest monsoon. *Mon. Wea. Rev.,* **108,** 1840–1853.

Tanaka, M., 1992: Intraseasonal oscillation and the onset and retreat dares of the summer monsoon over east, southeast Asia and the western Pacific region using GMS high cloud amount data. *J. Meteor. Soc. Japan,* **70,** 613–629.

Tao, S., and L.-X. Chen, 1987: A review of recent research on the east Asian summer monsoon in China. *Monsoon Meteorology,* C.-P. Chang and T. N. Krishnamurti, Eds., Oxford University Press, 60–92.

Ueda, H., T. Yasunari, and R. Kawamura, 1995: Abrupt seasonal change of large-scale convection activity over the western Pacific in northern summer. *J. Meteor. Soc. Japan,* **73,** 795–809.

Wang, B., 1994: Climatic regimes of tropical convection and rainfall. *J. Climate,* **7,** 1109–1118.

——, and H. Rui, 1990: Synoptic climatology of transient tropical intraseasonal convection anomalies: 1975–1985. *Meteor. Atmos. Phys.,* **44,** 43–62.

——, and Y.-H. Ding, 1992: An overview of the Madden–Julian oscillation and its relation to monsoon and mid-latitude circulation. *Adv. Atmos. Sci.,* **9,** 93–111.

——, and X. Xie, 1996: Low-frequency equatorial waves in vertically sheared zonal flow. Part I: Stable waves. *J. Atmos. Sci.,* **53,** 449–467.

Webster, P. J., 1972: The response of the tropical atmosphere to local study forcing. *Mon. Wea. Rev.,* **100,** 518–541.

——, and S. Yang, 1992: Monsoon and ENSO: Selectively interactive systems. *Quart. J. Roy. Meteor. Soc.,* **118,** 877–926.

Xie, X., and B. Wang, 1996: Low-frequency equatorial waves in vertically sheared zonal flow. Part II: Unstable waves. *J. Atmos. Sci.,* **53,** 3589–3605.

Yanai, M., and C. Li, 1994: Mechanisms of heating and the boundary layer over the Tibetan Plateau. *Mon. Wea. Rev.*, **122,** 305–323.

Yasunari, T., 1979: Cloudiness fluctuations associated with the Northern Hemisphere summer monsoon. *J. Meteor. Soc. Japan,* **57,** 227–242.

——, 1980: A quasi-stationary
appearance of 30–40-day period in the cloudiness fluctuation during the summer monsoon over India. *J. Meteor. Soc. Japan,* **58,** 225–227.

Zeng, Q.-C., B.-L. Zhang, Y.-L. Liang, and S.-X. Zhao, 1994: East Asian summer monsoon—A case study. *Proc. Indian Nat. Sci. Acad.,* **60A,** 81–96.

Zhu, B.-Z., 1988: Origin and properties of the east Asian summer monsoon. Preprint, *Int. Conf. on Tropical Meteorology,* Brisbane, Australia.

——, and B. Wang, 1993: The 30–60-day convection seesaw between the tropical Indian and western Pacific Oceans. *J. Atmos. Sci.,* **50,** 184–199.